Attenuation of High-Frequency *Lg* Waves around the Yangsan Fault area, the Southeast Korea

Tae-Woong Chung* and Kie-Hwa Lee**
*Department of Geoinformation Sciences, Sejong University
**School of Earth and Environmental Sciences, Seoul National University

ABSTRACT

The attenuation study of *Lg* waves is very important in the southeast Korea because the Yangsan fault, believed to be active faults, lies in the industrialized region of the area. By applying the reversed two-station method for the vertical component of the velocity seismogram, we first estimated the *Lg* attenuation coefficient in this area: $\gamma = (0.009 \pm 0.0005)\, f^{0.06 \pm 0.03}$ between 0.87 and 10 Hz. The Q_{Lg}^{-1} values converted from γ prove to be higher than those of S-waves, and show the highest values in the world for the high frequency part around 10 Hz. This high attenuation of *Lg* may be related to a block of *Lg* propagation near the East Sea and/or an undulately thinning crust of the studied area.

Key words: Attenuation, *Lg*, southeast Korea, the reversed two-station method, block of *Lg*

Tae-Woong Chung and Kie-Hwa Lee, 2002, Attenuation of High-Frequency *Lg* Waves around the Yangsan Fault area, the Southeast Korea. Journal of the Korean Geophysical Society, v. 5, n. 1, p. 1-8

요 약: 한반도 남동지역에서의 *Lg* 감쇠 연구는 산업 지역에 놓인 활성단층으로 여겨지는 양산단층의 존재로 매우 중요하다. 두 관측점법에 의한 *Lg* 감쇠를 해석한 결과, 0.87 - 10 Hz 구간이 $\gamma = (0.009 \pm 0.0005)\, f^{0.06 + 0.03}$ 이다. γ 값에서 변환된 Q_{Lg}^{-1} 값은 동일한 지역에서 측정된 S파의 값보다 매우 높고, 10 Hz 가까운 영역에서는 세계에서도 가장 높은 수준이 검출되었다. 이 높은 값은 동해에 의한 *Lg* 차단 효과이거나, 조사지역의 지각두께 변화와 연관이 된 것으로 보인다.

주요어: 감쇠, *Lg*, 한국 남동부, 두관측점법, *Lg* 차단

(Tae-Woong Chung, Department of Geoinformation Sciences, Sejong University, Seoul 143-747, Korea; chungtw@sejong.ac.kr; Kiehwa Lee, School of Earth and Environmental Sciences, Seoul National Universiyty, Seoul 151-742; kihwalee@plaza.snu.ac.kr)

1. Introduction

Since the *Lg* phase is commonly a dominant feature in the seismic wave field at regional distances, the attenuation of *Lg* is very important not only for seismological research but also purpose such as earthquake-resistant design in construction. This explains why numerous attenuation studies of *Lg* as well as S-waves have been undertaken world-wide, mainly in seismo-active zones and/or densely populated industrial areas (e.g. Frankel *et al.*, 1990; Kinoshita, 1994).

The Yangsan fault system in the southeast Korea has been receiving increasing attention because the fault lies in the industrial region where nuclear power plants are located (Fig. 1). The main fault trending NNE-SSW is about 200 km long and runs parallel with other subsidiary faults. These faults are located mainly in the area of Cretaceous sediments that were intruded by igneous rocks from the Cretaceous to the Tertiary (Chang, 1987). Right-lateral displacements of these faults took place in the early Quaternary (Sillitoe, 1977; Otsuki and Ehiro, 1978), and possibility for their recurrence is suggested (Lee *et al.*, 1984; Lee and Jin, 1991; Choi *et al.*, 1998).

Historically, the Yangsan fault is believed to be

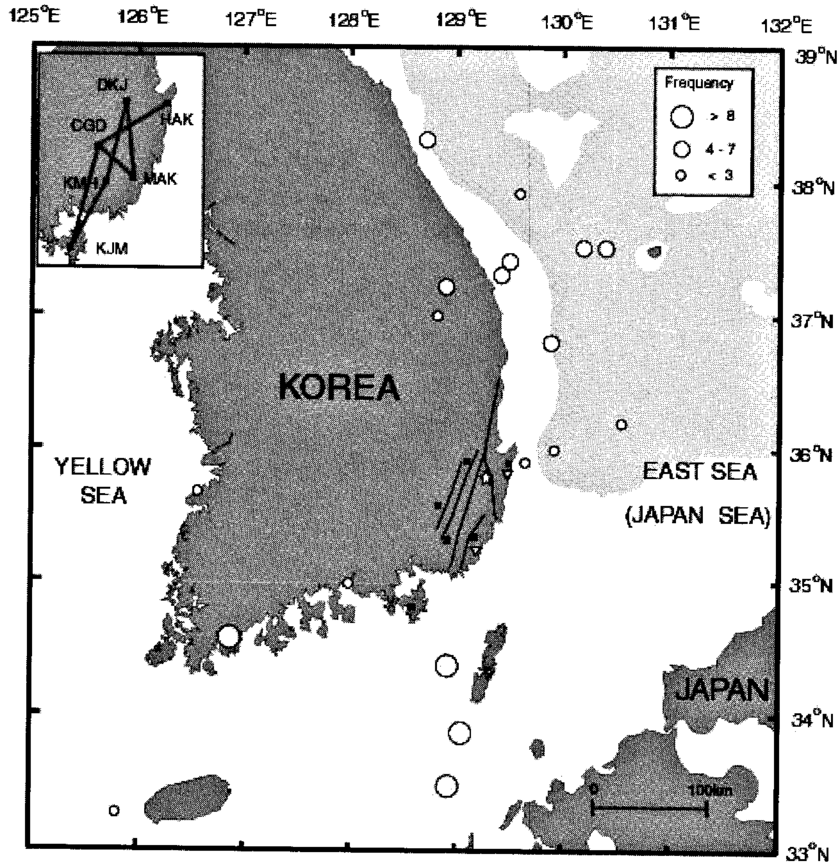

Fig. 1. Map of Korea showing seismic stations (solid squares), epicenters (open circles) of 19 earthquakes used in this study, and the Yangsan fault systems (solid lines). The frequency indicates how many times each event is used as combinations of RSTM. Reversed triangles denote atomic power plants, and an asterisk the epicenter of the earthquake of June 26, 1997 (M 4.3). The gray area represents the place deeper than 1000m bathymetry. The inset in the upper left shows the seismic stations of KIGAM with the abbreviation names. The lines connecting the station pairs are the path segments along which the *Lg* attenuation is measured.

responsible for a large earthquake that caused more than a hundred deaths in A.D. 779 (Lee, 1998). On June 26, 1997, an earthquake with magnitude (M) 4.3 occurred near the fault (star in Fig. 1), even though Korea is far from a seismically active plate boundary and earthquakes M 〉 4 have not frequently occurred in this century.

In the Yangsan fault area, a regional seismic network has been in operation by Korean Institute of Geology, Mining and Materials (KIGAM) since December, 1994 (< in Fig. 1). Based on the network data, Chung and Sato (2001) measured very low attenuation values for P- and S-waves by means of the coda-normalization method. In this paper, using the network data, we analyze the attenuation of *Lg* waves by the reversed two-station method.

2. Method of Analysis and Data

We estimate *Lg* attenuation by using the reversed two-station method (RSTM) proposed by Chun *et al.* (1987). If two stations and sources are linearly located as in Figure 2, RSTM calculates the attenuation coefficient γ and Q by following equation.

$$\frac{F(d_{1,2})}{F(d_{1,1})}\frac{F(d_{2,1})}{F(d_{2,2})} = \left(\frac{d_{1,2}}{d_{1,1}}\frac{d_{2,1}}{d_{2,2}}\right)^{-0.5} e^{-2\gamma\Delta}$$

where F denotes the spectral amplitude of the *Lg* wave, the epicentral distance from source i to station j, and

$\Delta = d_{1,2} - d_{1,1} + d_{2,1} - d_{2,2}$

$\gamma = \frac{\pi f}{QU}$, where f is the frequency, and U is the group velocity.

We selected 18 earthquakes for this study (Table 1). The origin time, hypocenter and magnitude of 13 events were determined by the Korea Meteorological Administration (KMA), whose stations are located throughout South Korea. The corresponding earthquake parameters for three events near Japan

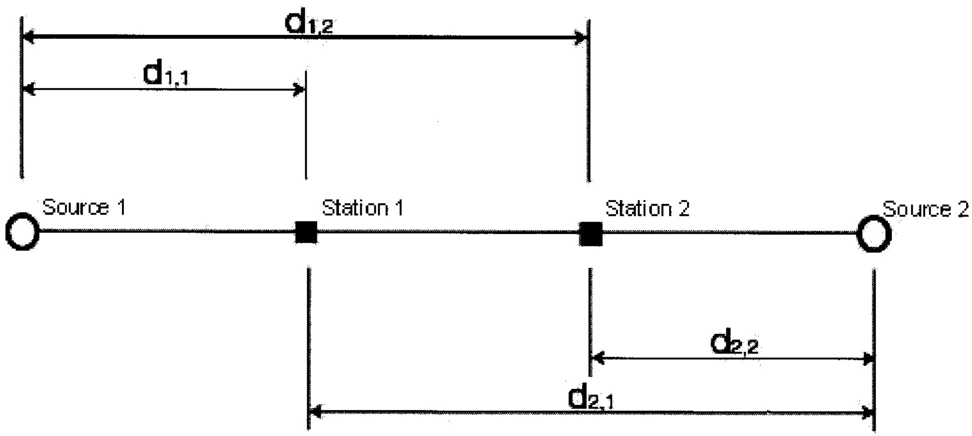

Fig. 2. Schematic figure showing the linear alignment of sources and stations for RSTM.

Table 1. Earthquakes. The frequency indicates how many times each event is used as combinations of RSTM.

Event No.	Date			Origin Time (Hr Min Sec)			Latitude (°N)	Longitude (°E)	Magnitude	Frequency
1	24	Jan.	1996	05	09	55	37.9	129.6	4.2	2
2	27	Feb	1996	04	39	34	35.9	129.6	2.6	1
*3	6	May	1996	07	46	40	33.9	129.0	3.1	8
4	3	Aug.	1996	00	06	59	37.4	129.5	2.7	6
5	15	Jan.	1997	05	34	05	38.3	128.7	3.2	6
6	2	Oct.	1997	23	47	19	35.0	128.0	2.4	1
*7	7	June	1998	17	39	28	34.4	128.9	3.1	11
*8	2	July	1998	05	52	46	33.5	128.9	3.5	8
9	7	July	1998	17	37	12	36.0	129.9	2.7	1
10	24	Jan.	1999	01	01	52	37.0	128.8	3.3	2
11	14	Mar.	1999	20	31	6	37.5	130.4	3.2	4
12	28	Mar.	1999	12	39	42	37.5	130.2	3.0	4
13	8	Apr.	1999	00	40	24	37.2	128.9	2.9	4
14	4	May	1999	03	09	50	37.3	129.4	2.5	4
#15	13	July	1999	13	52	59	36.2	130.5	2.7	1
#16	19	Mar.	2000	16	46	14	36.8	129.9	2.8	6
17	11	May	2000	10	51	18	33.3	125.9	3.1	1
18	29	Jan.	2001	11	44	9	35.7	126.6	3.0	2

* form JMA
\# form KiGAM

were obtained by the Japan Meteorological Administration (JMA); those of the last two were obtained by KIGAM. The epicentral distances range from 87 to 359 km, and the interstation path lengths range from 58 to 84 km. Almost events are repeatedly used for combinations of RSTM; the number of frequency is shown in Table 1 and Figure 1.

All analyses are based on short-period, vertical-component velocity recordings. The sampling rate of 7 records is 50/sec (corresponding to a Nyquist frequency of 25 Hz) and that of the remainder is 100/sec (Table 2). For the *Lg* record window, we carefully measured the onset time of each record as a starting point; measured group velocities ranged from 3.33 to 3.76 km/sec (Table 2). The ending point was fixed with 2.60 km/sec as a group velocity, which is compatible with those considered by others (Chun *et al.*, 1987; Campillo *et al.*, 1985). We removed a trend and mean value from each seismogram and applied a 5 % cosine taper to the

Table 2. Station pairs.

Event	Station		Lg Velocity (km/sec)		Epicentral Distance (km)		Azimuth (°)		interstation ditance
No.	Near	Far	Near	Far	Near	Far	Near	Far	(km)
1	*DKJ	MAK	3.51	3.52	195	256	152	158	61
2	KMH	KJM	3.57	3.59	114	176	230	222	62
3	*KMH	*DKJ	3.58	3.61	165	232	356	2	65
3	*MAK	*HAK	3.58	3.56	168	234	4	10	67
4	*DJK	*KMH	3.72	3.72	165	234	192	193	65
4	*DJK	MAK	3.72	3.73	165	227	192	187	69
5	DJK	KMH	3.71	3.70	264	329	172	177	62
5	DJK	MAK	3.71	3.68	264	328	172	173	65
6	CGD	HAK	3.39	3.55	102	171	49	53	64
7	KMH	DKJ	3.62	3.64	106	174	1	6	69
7	MAK	HAK	3.57	3.58	112	180	13	6	68
7	MAK	DKJ	3.57	3.58	112	174	13	6	62
8	KMH	DKJ	3.60	3.63	209	277	1	4	62
8	KJM	CGD	3.53	3.61	155	239	350	359	68
9	KMH	KJM	3.53	3.62	114	176	230	222	84
10	CGD	KJM	3.33	3.48	155	242	179	184	62
10	KMH	KJM	3.38	3.48	184	242	177	184	87
11	DKJ	KMH	3.56	3.61	208	274	214	209	57
12	DKJ	KMH	3.55	3.67	198	265	209	206	66
13	DKJ	KMH	3.49	3.65	141	206	172	179	67
14	DKJ	KMH	3.54	3.56	153	221	190	191	66
15	HAK	CGD	3.46	3.65	92	161	250	245	69
16	DKJ	KMH	3.48	3.55	121	187	214	207	69
16	HAK	MAK	3.41	3.52	107	176	198	201	68
17	KJM	KMH	3.76	3.68	301	359	56	51	58
18	CGD	HAK	3.51	3.54	204	264	93	85	60

*sampling rate is 50/sec

extra time of both ends of windowed data. The noise spectrum is also computed from the time window having the same length of *Lg* window preceding the Pn arrival.

We can form 26 one-way interstation passages whose source-station azimuthal difference is within 10°. From these passages, 36 combinations of 6 interstation paths are possible for RSTM (Table 3).

3. Measurements of *Lg* attenuation

We smoothed the data once with a simple running average over a frequency interval $\delta f = \pm 0.234$ Hz, and plotted 36 observations of $\gamma(f)$ between 0.6 and 30 Hz (Fig. 3). Several studies (e.g. Chun et al., 1987; Shin and Herrmann, 1986), however, restricted *Lg* study below 10 Hz frequency because of contamination by *Sn* at high frequencies. Since Figure 4 shows dispersed values above 10 Hz, we also restricted our study below 10 Hz.

We applied a simple weighting scheme, such that the weights assigned to γ values are directly proportional to the interstation path length, and obtained averaged γ values for all observations (Fig. 4). The methods of smoothing and weighting are the same

Table 3. Combinations. The number in parentheses indicates the frequency of each station closest to the source.

Combination No.	Stations	Events	Average Interstation Distance(km)
1-7	KMH(3)-DKJ(7)	3-4, 3-5, 3-11, 3-12, 3-13, 3-14 3-16	67
8-14		7-4, 7-5, 7-11, 7-12, 7-13, 7-14 7-16	
15-21		8-4, 8-5, 8-11, 8-12, 8-13, 8-14 8-16	
22-24	MAK(2)-DKJ(3)	3-1, 3-4, 3-5	63
25-27		7-1, 7-4, 7-5	
28-31	KJM(1)-KMH(3)	17-2, 17-9, 17-10	60
32-33	HAK(1)-CGD(2)	15-6, 15-24	66
34-35	HAK(1)-MAK(2)	16-3, 16-7	67
36	KJM(1)-CGD(1)	8-10	85

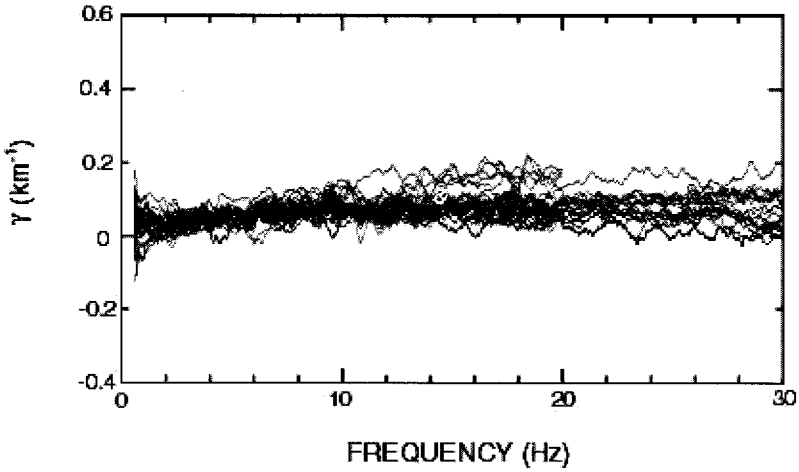

Fig. 3. g(f) values for the 36 combinations (Table 1) from 26 individual interstation passages (Table 2). The records with 50 samples/sec were measured within 20 Hz.

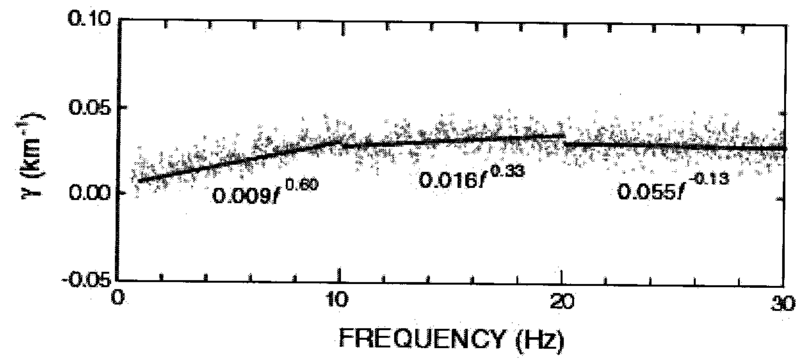

Fig. 4. Averaged γ(f) values of Figure 3. Solid curves for each frequency range represent the calculated maximum-likelihood fits with applying weights.

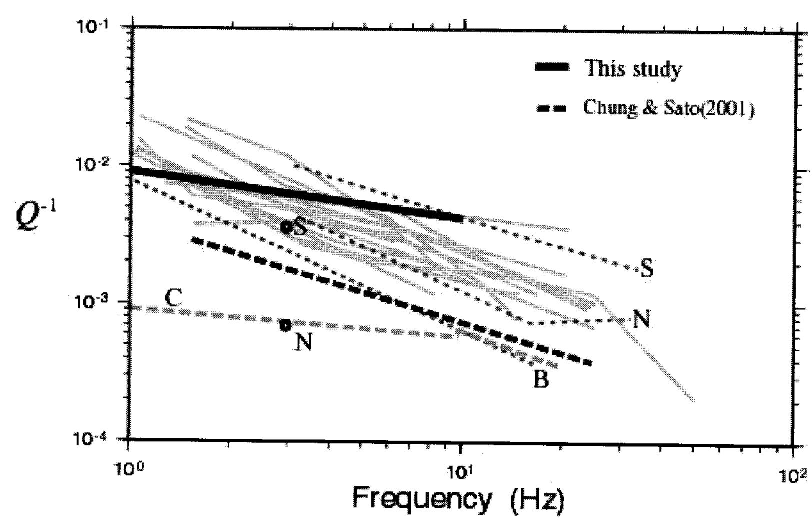

Fig. 5. Comparison of Q^{-1} with other studies. Thick solid line denotes Q^{-1} of Lg converted from g of this study. Dashed line refer to Q^{-1} of S-wave for the same area (Chung and Sato, 2001). A gray dashed line denoted by C refers to the study in Canadian Shield area (Chun *et al.*, 1987). Open circles and dotted lines designated by S, N refer to *Lg* and S-wave study in southern California, and New York State (Frankel et al., 1990), respectively. The dotted line indicated by B refers to the study in Baltic shield (Kvamme and Havskov, 1989). Gray lines show the reported measurements in the world (modified from Sato and Fehler, 1998).

as those of Chun *et al.* (1987).

Chun *et al.* separately fit γ by using a maximum-likelihood method with a form of αf^{β} where α and β are constants from 0.6 to 10 Hz. Our lower bound has changed from 0.6 to 0.87 Hz because of the negative value of averaged γ. The values thus derived are of the form $\gamma = (0.009 \pm 0.0005) f^{0.06 \pm 0.03}$ (solid lines in Fig. 4).
Since the group velocity for *Lg* is generally close to 3.5 km/sec (see e.g. Campillo, 1990), we set the group velocity U to be 3.5 km/sec, and obtain values $Q_{Lg}^{-1} = (0.011 \pm 0.0005) f^{-0.40+0.03}$ (Fig. 5).

4. Discussion

For comparison, Q_S^{-1} values of several areas of the world are shown by shaded lines in Figure 5.

These values are measurements on the ground for similar crustal depth range with hypocentral distances between 90 and 400 km (e.g. Sato and Fehler, 1998). Frankel *et al.* (1990) observed a remarkable difference of Q_S^{-1} between New York State and southern California (dotted lines), which are seismically inactive and active regions respectively. They also reported such a difference for Q_{Lg}^{-1} for *Lg* at 3 Hz (○ in Fig. 5). For the southeast Korea, Chung and Sato (2001) derived very low Q^{-1} of S-waves from the data with a hypocentral range between 40 and 160 km (bold broken line). This is close to that for the Baltic shield (Kvamme and Havskov, 1989), which is seismically rather stable, and is also very low among the Q_S^{-1} values reported (the lowest dotted line). The low Q_{Lg}^{-1} in the Canadian Shield area (Chun *et al.*, 1987) reflects seismic stability. In our study, the Q_{Lg}^{-1} values are higher than those of S-waves. For the high frequency part around 10 Hz, our Q_{Lg}^{-1} values are among the highest in the reported values of the world.

The block of *Lg* propagation near the East Sea (Japan Sea), which has a typical oceanic crust seems to be related. Furumura and Kennett (2001) show blockage of *Lg* for the oceanic crustal region deeper than the 1000-m contour. Our right side of the two point data is located near the 1000-m contour region of the East Sea.

The gravity study by Choi (1988) indicates that the Moho depth in the studied area is significantly shallowed on the seaside (Fig. 6). This undulately thinning crustal structure may also be one cause of the large attenuation of *Lg*.

5. Conclusion

The attenuation study of *Lg* waves is very important in the southeast Korea because active faults lie in

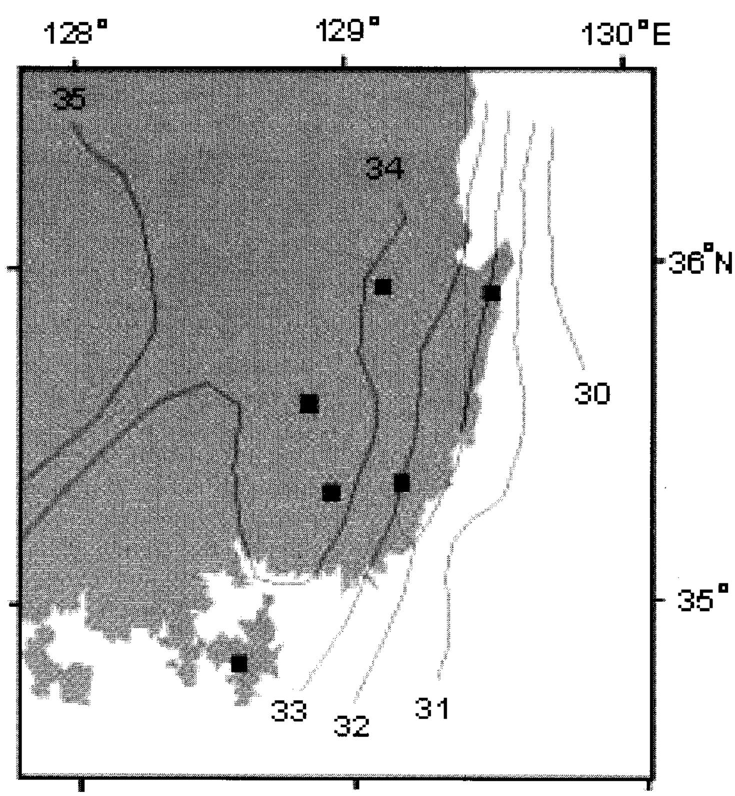

Fig. 6. Map of the Moho depth with 1-km contour interval (modified from Choi, 1987).

the industrialized region of the area. The estimated *Lg* attenuation coefficient by RSTM is $\gamma = (0.009 \pm 0.0005) f^{0.06 \pm 0.03}$ between 0.87 and 10 Hz. The Q_{Lg}^{-1} values converted from γ prove to be higher than those of S-waves, and show the highest values in the world for the high frequency part around 10 Hz. This high attenuation of *Lg* may be related to a block of *Lg* propagation near the East Sea and/or an undulately thinning crust of studied area.

Acknowledgements

This paper was accomplished with Research Fund No. 006109 provided by the Ministry of Science & Technology, and was partly supported by grant No. R01-1999-00314 from the Korean Science & Engineering Foundation.

References

Campillo, M., 1990, Propagation and attenuation characteristics of the crustal phase *Lg*., Pure and Applied Geophysics, 132, 1-9.

Campillo, M., J. L. Plantet and M. Bouchon, 1985, Frequency-dependent attenuation in the crust beneath central France from Lg waves: data analysis and numerical modeling, Bulletine of the Seismological Society of America, 75, 1395-1412.

Chang, K. H, 1987, Cretaceous strata: in D. S. Lee Ed., Geology of Korea, Kyohak-Sa Pub. Co., Seoul, 175- 193.

Choi, G.S., 1987, Gravity and crustal structure, in D. S. Lee Ed. Geology of Korea, Kyohak-Sa Pub. Co., Seoul, 264-269.

Choi, U., D.Y. Lee, B. J. Lee, C. R. Ryoo, P. Y. Choi, S. J. Choi, D. L. Cho, J. Y. Kim, C. B. Lee, W. S. Kee, D. Y. Yang, I. J. Kim, Y. Kim, J. H. Yoo, B. G. Chae, W. Y. Kim, P. J. Kang, I. H. Yu, and H. K. Lee, 1998, An investigation and evaluation of capable fault - southeastern part of the Korean Peninsula, KIGAM Research Report, KR-98(C)-22 (in Korean).

Chun, K. Y., G. F. West, R. J. Kokoski, and C. Samson, 1987, A novel technique for measuring *Lg* attenuation: results from Eastern Canada between 1 to 10 Hz, Bulletine of the Seismological Society of America, 77, 398-419.

Chung, T.W., and H. Sato, 2001, Attenuation of high-Frequency P- and S-waves in the crust of the southeastern Korea, Bulletine of the Seismological Society of America, 91, 1867-1874.

Frankel, A., A. McGarr, J. Bicknell, J. Mori, L. Seeber and E. Cranswick, 1990, Attenuation of high-frequency shear waves in the crust: measurements from New York State, South Africa and Southern California, Journal of Geophysical Research, 95, 17441-17457.

Furumura, T., and B.L.N. Kennett, 2001, Variation in regional phase propagation in the area around Japan, Bulletine of the Seismological Society of America, 91, 667-682.

Kinoshita, S., 1994, Frequency-dependent attenuation of shear waves in the crust of the southern Kanto area, Japan, Bulletine of the Seismological Society of America, 84, 1387-1396.

Kvamme, L. B., and J. Havskov, 1989, Q in southern Norway, Bulletine of the Seismological Society of America, 79, 1575-1588.

Lee, K., 1998, Historical earthquake data of Korea, Journal of the Korean Geophysical Society, 1, 3-22 (in Korean).

Lee, K., B. I. Jeong, Y. H. Kim, and S. J. Yang, 1984, A geophysical study of the Yangsan fault area, Journal of the Geological Society of Korea, 20, 222-240.

Lee, K., and Y. G. Jin, 1991, Segmentation of the Yangsan fault system: Geophysical studies on major faults in the Kyeongsang basin, Journal of the Geological Society of Korea, 27, 434-449.

Otsuki, K. and M. Ehiro, 1978, Major strike-slip faults and their bearing on spreading in the Japan Sea, Journal of Physics of the Earth, 26 (supplementary), 537-555.

Sato, H. and M. C. Fehler, 1998, Seismic wave propagation and scattering in the heterogeneous earth, Springer-Verlag New York, Inc.

Shin, T. C. and R. B. Herrmann, 1983, Regionalization of crustal coda Q in the continental United States, Journal of Geophysical Research, 88, 527-538.

Sillitoe, R. H., Metallogeny of an Andean type continental margin in South Korea, 1977, Implications for opening of the Japan Sea, in M. Talwani and W.C. Pitman III Eds., Deep Sea Trenches and Back Arc Basins, Maurice Ewing Series, 1, American Geophysical Union, Washington, D.C., 303-310.

2002년 1월 4일 원고접수
2002년 3월 25일 원고채택